Available online at www.sciencedirect.com
SCIENCE DIRECT®
Journal of Power Sources 127 (2004) 264–272
JOURNAL OF POWER SOURCES
www.elsevier.com/locate/jpowsour

Long term investigations of silver cathodes for alkaline fuel cells

N. Wagner*, M. Schulze, E. Gülzow

Deutsches Zentrum für Luft und Raumfahrt (DLR), Institut für Technische Thermodynamik, Pfaffenwaldring 38-40, D-70569 Stuttgart, Germany

Abstract

Alkaline fuel cells (AFC) are an interesting alternative to polymer electrolyte fuel cells (PEFC). In AFC no expensive platinum metal is necessary; silver can be used for the oxygen reduction reaction (ORR) (cathode catalyst). For technical use of AFC the long term behavior of AFC components is important, especially that of the electrodes. The investigated cathodes for AFC consist of a mixture of silver catalyst and polytetrafluorethylene (PTFE) as organic binder rolled onto a metal web. The electrodes were electrochemically investigated through measuring *V–i* curves and electrochemical impedance spectroscopy (EIS). The electrochemical characterization and the long term tests were performed in half-cells at 70 °C using pure oxygen (1 bar) under galvanostatic conditions. The cathodes were electrochemically investigated in half-cells using reference electrodes (Hg/HgO) by periodically recording *V–i* curve and electrochemical impedance spectroscopy. In addition, the cathodes were physically characterized by scanning electron microscopy (SEM) and X-ray photoelectron spectroscopy (XPS).

Keywords: Alkaline fuel cell; Gas-diffusion electrode; Oxygen reduction reaction; Silver cathode; Degradation; Scanning electron microscopy; X-ray photoelectron spectroscopy

1. Introduction

Low temperature fuel cells like polymer electrolyte fuel cells (PEFC) and alkaline fuel cells (AFC) represent important elements in pollution free energy supply for mobile applications. Alkaline fuel cells are an interesting alternative to polymer electrolyte membrane fuel cells. A review of the state of the art of alkaline fuel cell is given in [1]. In AFC no expensive platinum metal is necessary. However, for technical use of AFC the long term behavior of AFC components is important, especially that of the electrodes. Nickel can be used for the hydrogen oxidation reaction (catalyst in the anode) and on the cathode silver can be used as catalyst, because the alkaline electrochemical environment in AFC is less corrosive compared to acid fuel cell conditions. In addition, a liquid alkaline solution is used as electrolyte. Both, catalysts and electrolyte, represent a big cost advantage with AFC in comparison to PEFC and, therefore, considering only the cost, the AFC has a much higher potential for the commercialization of fuel cells. Nevertheless, very recently a fuel cell company specialized on AFC finished its activity [2]. The advantages of AFC are not restricted only to the cheaper components, AFC has also advantages in the system technique, because no process gas humidification is needed for AFC operation, which is a significant problem of the present PEFCs, and due to the fact that the electrolyte is liquid the temperature management of AFC can be performed with the electrolyte. It may be seen that a liquid electrolyte is disadvantageous, because AFC needs a circuit for the electrolyte; but a similar circuit for liquids is also necessary for high efficiency PEFC systems for temperature management, although the electrolyte circuit in AFC may be more expensive because of the higher corrosivity of the electrolyte compared with water of other cooling media in the PEFC. The alkaline solution in the AFC must be reconcentrated during long term operation, but this is very simple in comparison to the water management in a PEFC.

The life time of fuel cells is a decisive factor for their commercialization. Therefore, the degradation of fuel cell components is under increased investigation and mainly focused on PEFC [3–14]. For alkaline fuel cells several studies of degradation processes exist [15–25], they are all focussed on the electrodes, because the electrolyte in AFCs can be easily exchanged. In the case of using the silver gas-diffusion electrode (GDE) in a complete alkaline fuel cell, the solubility of silver can lead in certain circumstances to a transfer of silver to the anode and the resulting plating out may damage the catalysts (usually Raney–Nickel) of the anode. On open circuit standing the oxidation of silver may occur. Especially carbon-containing cathodes are suffering from oxidation at

* Corresponding author. Tel.: +49-711-6862-631; fax: +49-711-6862-322.
E-mail address: norbert.wagner@dlr.de (N. Wagner).

0378-7753/$ – see front matter © 2003 Elsevier B.V. All rights reserved.
doi:10.1016/j.jpowsour.2003.09.022

higher temperatures. Shut down and restarting procedures can lead to damage too.

This paper deals with the investigation of the degradation of silver gas-diffusion electrodes during oxygen reduction reaction (ORR) at constant load.

2. Experimental

2.1. Electrodes

The physical and electrochemical investigations were performed on polytetrafluorethylene (PTFE)-bonded gas-diffusion silver electrodes (GDEs) during and after the oxygen reduction reaction in alkaline solution. The investigations arise from fundamental and practical interests [26]. Oxygen reduction electrocatalysis is of special importance for fuel cells [27], metal–air batteries and industrial chlorine-alkali electrolysis as well. Silver is a known electrocatalyst for the reduction of oxygen in alkaline fuel cell cathodes. To enhance this catalytic activity, silver is used in a form with high specific area such as porous electrodes where the silver particles are dispersed in the porous matrix. The porous PTFE-bonded gas-diffusion electrodes used in this work were prepared by a cold rolling process [28]. They consist of the electrocatalytic powder (silver or silver oxide), the organic binding agent (PTFE) and a metal wire gauze to stabilize mechanically the electrode and to collect the current. In gas-diffusion electrodes hydrophobic and hydrophilic pore systems are required. In AFC the hydrophilic system allows the penetration of the electrolyte into the electrode and the transport of the ions to or from the reaction zone; the hydrophobic pore system is required for the transport of the oxygen to the reaction zone. In addition to give the mechanical stability, the PTFE in the electrodes forms a hydrophobic pore system, whereby the spider web of PTFE fibers in and on the electrodes are formed during preparation.

The working electrodes were circular PTFE-bonded gas-diffusion silver electrodes (GDEs) with an apparent geometric surface area of 1 cm^2. The thickness of the electrodes was 0.4 mm. These electrodes were produced by electrochemical reduction of silver oxide GDE. The reduction of the silver oxide electrode (1) was performed galvanostatically at 6.7 mA cm^{-2} (referred to geometric surface area) in 30 wt.% KOH at 50 °C, corresponding to the following equation:

$$Ag_2O + H_2O + 2e^- \rightarrow 2Ag + 2OH^- \quad \text{with}$$
$$E^0 = 247\,\text{mV versus Hg/HgO} \qquad (1)$$

During the reduction the electrode potential was measured versus the reference electrode (Hg/HgO with 926 mV versus NHE). At the beginning, the open circuit potential (OCP) was around 220 mV and the reduction of the silver oxide was completed reaching −114 mV during polarization (Fig. 1). From the integral $\int i\,dt$, 47 mg Ag cm^{-2} was calculated. By further polarization of the electrode the reduction of an additional oxide takes place. The reduction of the electrode was completed reaching −500 mV (hydrogen evolution) during polarization.

The counter electrode was a Pt-foil. All potentials are referred to the Hg/HgO reference electrode. Electrolyte solutions were prepared from analytical grade reagents (Merck).

2.2. Electrochemical cell and electrochemical measurements

The electrochemical performance was measured by periodically recording of *V*–*i* curves. The long term tests were performed for more than 2500 h. In addition, in a long term test one electrode was characterized after different operation times at 100 mA cm^{-2} by electrochemical impedance spectroscopy (EIS) at open circuit potential. The experiments were carried out in a polymethylmethacrylate half-cell

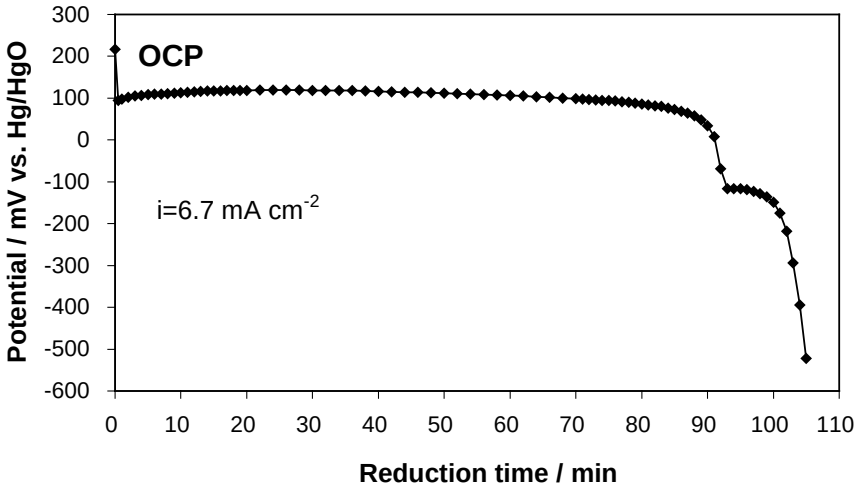

Fig. 1. Electrode potential during electrochemical reduction of silver oxide GDE at 6.7 mA cm^{-2} in 30 wt.% KOH at 50 °C.

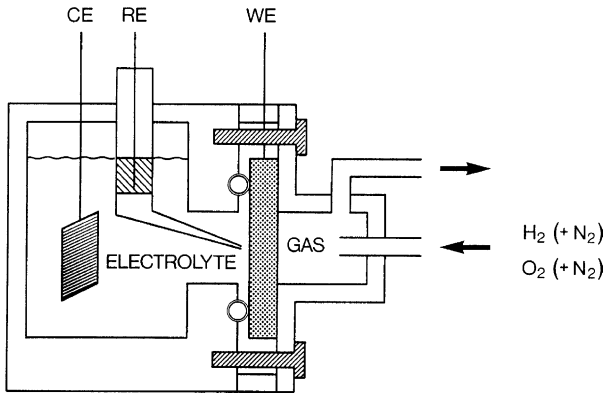

Fig. 2. Schematic diagram of the plexi-glass cell used for electrochemical measurements.

(Fig. 2) with two chambers, a gas chamber and an electrolyte chamber, which are kept tightly together by four screws. The gas chamber has inlet and outlet for the gas flow, while the electrolyte chamber has connections for filling and draining the electrolyte. The working electrode (GDE) was placed between these two chambers and fixed with a sealing rubber. The whole assembly was placed in a thermostated water bath for carrying out experiments at different temperatures. An EG&G potentiostat (model 273) was used for the steady state and cyclic voltammetric measurements. Electrochemical impedance spectra in the frequency range 1 mHz to 64 kHz were obtained using a Solartron frequency response analyzer (FRA 1250) integrated in a computer system. The further evaluation of the measured EIS was performed with the IM6 simulation program of Zahner-elektrik. For recording and monitoring the electrochemical data from the long term experiments, a computer controlled experimental set-up containing nine half-cells is available [29]. Thus it is possible to adjust the load of the electrodes and keep it constant and to record stationary cell characteristics with IR-drop corrections.

2.3. Physical characterization

In addition to the electrochemical experiments, electrodes were characterized by physical methods before and after operation by scanning electron microscopy (SEM) and X-ray photoelectron spectroscopy (XPS) [30]. For this the electrodes were split into several parts for the different applied characterization methods. An investigation of the pore systems of the cathodes with nitrogen adsorption results in low pore volume values for analysis and an investigation with mercury penetration is impossible due to the formation of amalgam.

Prior to the physical characterization all electrodes were rinsed with distilled water and dried. For the SEM and EDX analyses the samples were dried in air, for XPS they were dried at reduced pressure conditions at elevated temperature for 8 h.

The electrodes were investigated by scanning electron microscopy to see the structure of the electrodes and the changes of the structure induced by the electrochemical stressing. The SEM/EDX measurements were performed with a TOPCON DS130 and a Zeiss Gemini LEO microscope equipped with a NORAN VOYAGER 3000 EDX-system. The microscope beam energy can be varied in the range of 1–40 keV, the maximum resolution of the SEM is 3 nm. The EDX analyzer has an ultra-thin window, allowing light element analysis from carbon upwards.

The XPS characterization of the electrodes was performed in a standard UHV chamber equipped with an XP-spectrometer (spherical analyzer $r = 127$ mm, 300 W X-ray tube with Al and Mg excitation) and a quadrupole mass spectrometer. The residual pressure in the analysis chamber was approximately $p \approx 4 \times 10^{-10}$ mbar. The composition of the residual pressure gas was controlled by a mass spectrometer. The pressure increased by nearly two orders of magnitude after transferring the GDE sample into the UHV chamber. By alternating steps of XP spectra measurement and ion etching of the surface depth profiles were recorded. During depth profiling of GDEs the etching period was increased after ten cycles. The changes of the surface composition during the depth profiling are not only induced by the etching of the surface, but also by the decomposition of the polymer induced by the ionizing irradiation [20]. The experimental conditions, drying temperature and time, X-ray doses and Ar^+ ion doses during the ion etching, were kept constant for all samples.

3. Results

3.1. V–i characteristics

For an exemplary illustration of the *V–i* characteristic, the first *iR*-corrected *V–i* curve is shown in Fig. 3. To quantify the degree of degradation of the silver gas-diffusion electrode during the oxygen reduction at 100 mA cm^{-2} the *iR*-corrected electrode potential was recorded. Starting from an *iR*-corrected electrode potential of −47 mV at 100 mA cm^{-2} the electrochemical performance of the used silver cathodes decreases during the operation time with a constant rate of approximately 20 μV h^{-1}.

3.2. XPS and SEM measurements

Surface science methods are used to determine the structure and chemical composition of the unused and the electrochemical stressed cathodes. Fig. 4 shows the depth profiles of an unused and an used cathode. In principle the depth profiles of both electrodes, used and unused, agree. At the beginning of the depth profile measurements a high concentration of the carbon and fluorine and a low concentration of the silver is observed. The fluorine and the carbon signal can be related to PTFE. A part of the carbon signal is

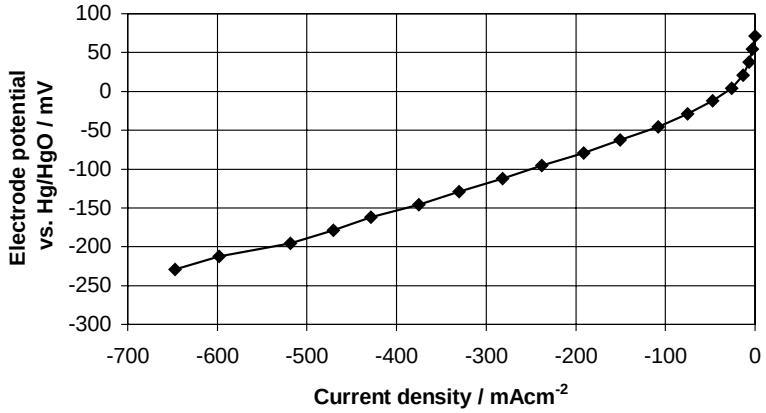

Fig. 3. First *iR*-drop corrected *V*–*i* curve of a new silver GDE during oxygen reduction at 70 °C in 30 wt.% KOH.

also related to PTFE decomposition products. Due to the ion etching the concentration of the fluorine decreases, whereas the carbon concentration and the silver concentration, too, increase. The PTFE is decomposed by the ionizing effect of the ion etching as well as by the X-rays, whereby fluorine rich fragments are evaporated [20]. In addition, the PTFE forms a thin film on the electrode surface, and this film is also removed by the ion etching. Consequently, the fluorine concentration decreases. On the other hand, the carbon of the PTFE is enriched on the electrode surface due to the PTFE decomposition. In addition, the efficiency of ion etching process for carbon is lower than for fluorine or for most other elements. As a result of the removing of the PTFE film from the electrode surface the silver concentration increases.

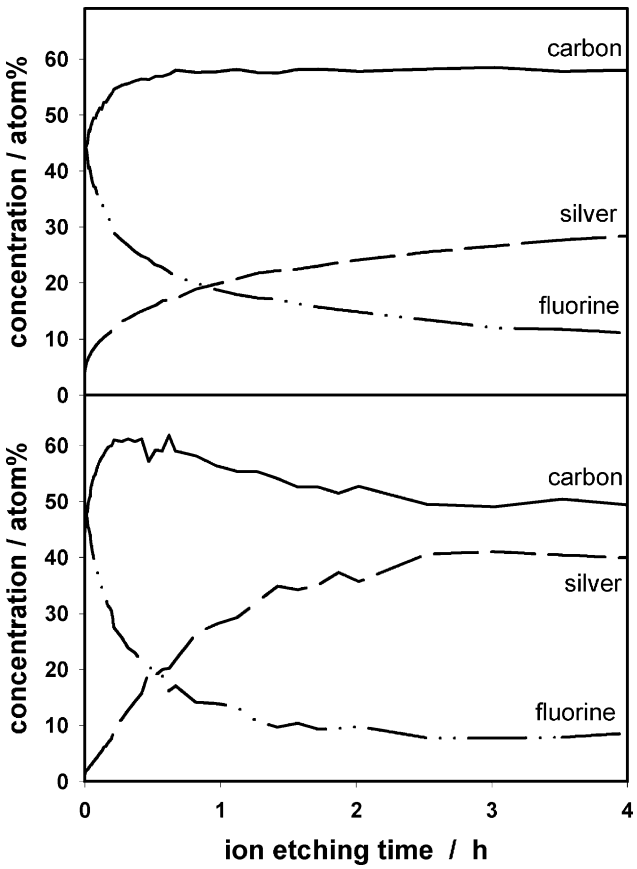

Fig. 4. XPS depth profile measurements of an unused silver cathode (top) and an used cathode (bottom). The used electrode was operated for 1344 h at 100 mA cm^{-2}.

The characteristic of the depth profiles is typical for electrodes prepared by the rolling technique and composed of a metallic catalyst and PTFE without carbon black. As a result of the rolling process a PTFE film on the surface is formed, which covers the metallic catalyst [23]. In the depth profiles of such electrodes a decrease of the fluorine signal and an increasing signal of the metallic catalyst is typically observed. The depth profiles of nickel anodes prepared with the rolling technique are described in [25].

Due to electrochemical operation the chemical composition is changed. The PTFE in the electrode is partially decomposed, which can be seen in the depth profile of the electrochemically stressed electrode by the enhanced decrease of the fluorine concentration. Similarly, an electrochemically induced decomposition of PTFE is also observed for other low temperature fuel cell electrodes like AFC or PEFC anodes [25,30,31]. The second difference in the depth profiles is the increased silver concentration. This is induced by the decomposition of the PTFE and the resulting lower concentration of the elements related to PTFE. The decomposition of the PTFE changes the hydrophobic/hydrophilic behavior and in this way it affects directly the three phase zone between catalyst, electrolyte and gas phase relevant for the reaction. Typically, the decomposition of PTFE reduces the hydrophobic property and so the electrode will be more flooded by the liquid electrolyte. Consequently the gas transport in the electrode is more hindered. In addition, the thickness of the three phase zone will be reduced.

In order to investigate the structure the cathodes were investigated by scanning electron microscopy. In Fig. 5 SEM-micrographs of unused and used silver gas-diffusion electrodes are shown. The SEM-micrographs were imaged in two different modes; first by the back-scattered electrons and second by using the secondary electrons. In both

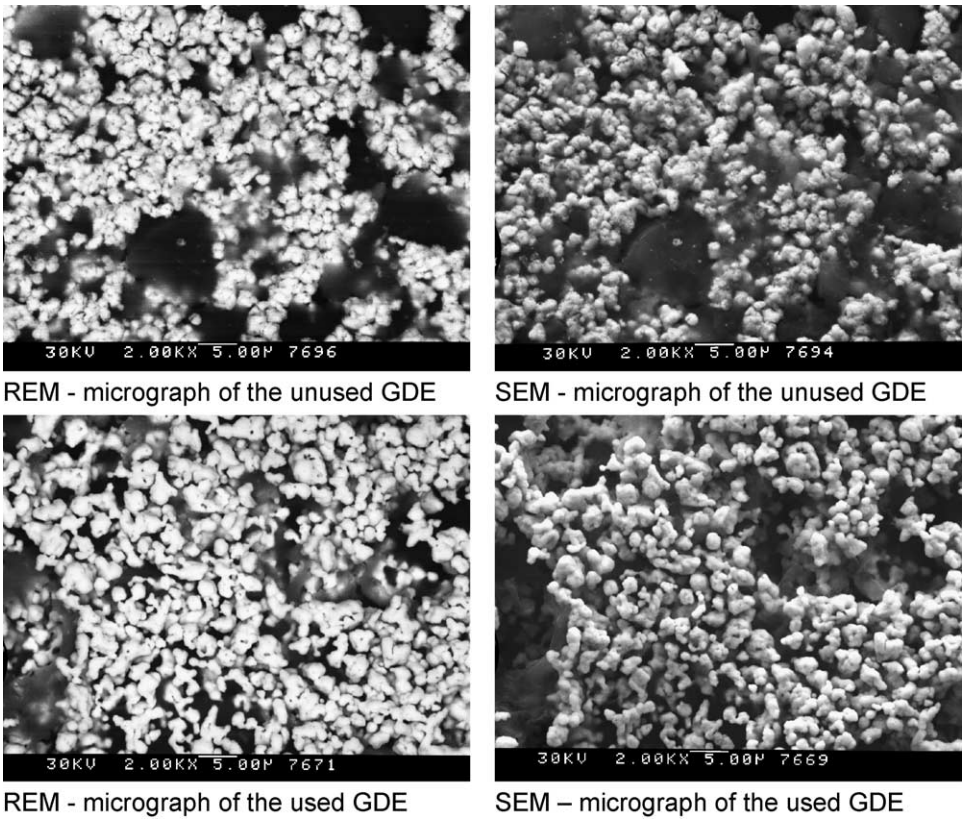

Fig. 5. REM-micrographs (left) of an unused silver GDE (top) and an used silver GDE (bottom), SEM-micrographs (right) of an unused silver GDE (top) and an used silver GDE (bottom).

imaging modes a material contrast is used. Heavy elements are more efficient for the back-scattering of electrons, therefore, the heavy elements are imaged more brighter than the lighter elements. The back-scattered electrons have a high energy. Consequently the electron mean free path is high [32] and the surface sensitivity is low. Typically, the back-scattered electrons are detected under a small angle to the sample normal. Therefore, the images are not influenced by shadow effects; consequently the images yield no steric effect.

Due to imaging by the secondary electrons the material contrast is caused by different work functions. Components with a low work function emit more electrons than components with a high work function and consequently they are imaged brighter. In addition, the secondary electrons have a lower energy than the back-scattered electrons, therefore the surface sensitivity is higher in the imaging mode, especially, if primary electrons with a low energy (low beam voltage) are used for the imaging. In addition to the differences in the material contrast and the surface sensitivity, the images were generated with electrons emitted or scattered in different angles. The secondary electrons are typically detected under a higher angle to the sample normal. As consequence the image of the sample generated with the secondary electrons is influenced by shadow effects of the topography. Therefore these micrographs show a more steric effect.

In both imaging modes used the silver is imaged bright and the PTFE dark, because the PTFE consists only of fluorine and carbon, which are both lighter elements, and in addition, the PTFE is an electrical insulator and has consequently a high value for the work function. In contrast, the silver atoms are significantly heavier and the work function is lower than for the PTFE. The SEM-micrographs imaged in both modes show the same differences for both electrodes, the unused and the used cathode. The alteration of the chemical composition observed in the XPS depth profiling does not effect a difference in the SEM images, whereby the information about the chemical composition, which can be derived by SEM are less than can be derived by XPS. By comparing the SEM images of the unused and the used electrodes one can see that the rough surface of the silver catalyst in the unused electrode becomes more flat due to the electrochemical stressing. A reduction of the roughness caused by electrochemical operation is reported for different noble metals like gold and platinum [33–40]. The decrease of the roughness is induced by the mobility of the catalyst atoms on the electrode surface. In contrast to other catalysts a change of the catalyst size by electrochemical stressing [40,41] is not observed for the silver cathodes.

As consequence of the decrease of the surface roughness the catalyst surface area decreases, too; simultaneously the pore system changes. The depth of the pores decreases. As

result of the alteration of the pore system the electrochemical behavior is influenced, whereby the geometrical surface of the electrodes keeps constant. The loss of the catalyst surface area is focused on the surface area at the end of the pores. Because the transport of the media, especially the transport of the electrolyte, to the end of the pores is more hindered than to all other surface areas in the electrode, the loss in the electrochemical performance should be not very strong.

3.3. Electrochemical impedance measurements

The ac impedance method was applied by several investigators [42–45] for the analysis of electrochemical reactions on porous electrodes. The electrode impedance was measured with an ac voltage signal in the frequency range 1 mHz to 64 kHz superimposed on the dc polarization potential. The amplitude of the ac signal was kept smaller than 10 mV peak-to-peak in order to maintain the current response within a linear range.

In order to analyze in detail the degradation (aging) process of silver electrodes during oxygen reduction, electrochemical impedance spectroscopy has been performed. The silver GDE has been operated at 100 mA cm^{-2} over 1400 h and impedance spectra were recorded at the open circuit potential, daily at the beginning and after 2 weeks of operation in 48 and 72 h intervals, respectively. Impedance spectra are represented as Bode plots (Fig. 6), where the logarithm of impedance magnitude $|Z|$ and the phase-shift (α) are plotted versus the logarithm of the frequency (f), or as Nyquist plots (Fig. 7), where the imaginary part of the impedance is plotted versus the real part of the impedance. Figs. 6 and 7 show that the impedance spectra change during operation at 100 mA cm^{-2}. During the measurement period of each impedance spectrum at OCP the electrode state stays

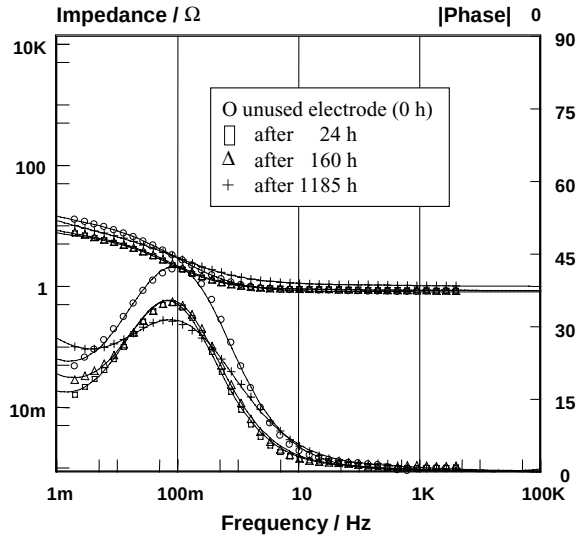

Fig. 6. Bode diagram ($\log|Z|$ vs. $\log f$) of the impedance spectra of the silver GDE measured at OCP, 70 °C, in 30 wt.% KOH during oxygen reduction at different times of operation at 100 mA cm^{-2}.

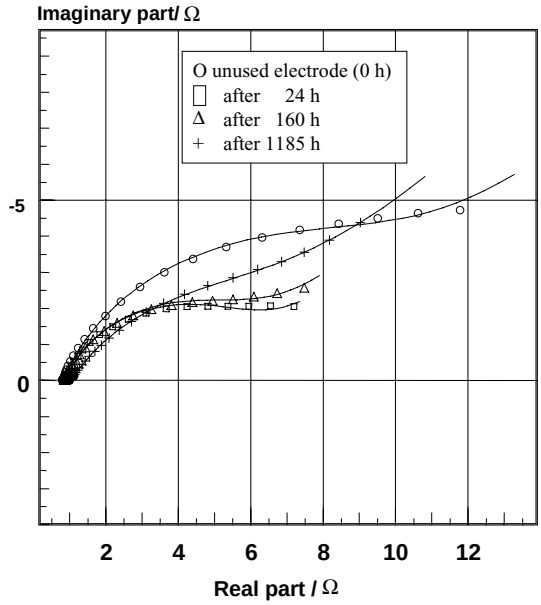

Fig. 7. Nyquist diagrams of the impedance spectra of the silver GDE measured at OCP, 70 °C, in 30 wt.% KOH during oxygen reduction after different times of operation at 100 mA cm^{-2}.

constant, the electrode degrades only during operation at 100 mA cm^{-2}. The first spectrum (0 h), recorded prior to the beginning of the long term operation differs from the EIS recorded after loading. During load, at first, the electrode is activated (second spectrum recorded after 24 h) and a slight change with operation time can be observed.

In order to evaluate the measured impedance spectra and to obtain kinetic data of the oxygen reduction reaction and to get findings about degradation during long term operation, the reaction steps have to be translated into an appropriate equivalent circuit which contains various impedance elements representing the involved reaction steps. These elements are generally represented as ohmic, capacitive or inductive components with particular dependencies of their complex impedance upon the frequency of the ac signal. The particular linking of these impedance elements described by an equivalent circuit is based upon the relationship between the processes represented by these elements. Subsequently occurring steps are represented by a series connection of the elements while steps occurring simultaneously are represented by a connection in parallel. In the case of porous electrodes the connection of the elements is more complicated.

The main features of the impedance measurements can be explained using the cylindrical pore model proposed by Göhr and others [46,47]. In this model the cylindrical pore is considered as a transmission line made of a large number of infinitesimally thin sections, with impedance elements for ground surface of pores, electrolyte in the pores, wall surface of pores, porous layer and surface layer. Taking into account only the pore electrolyte resistance (R_{por}) and the pore wall impedance, then the porous electrode model and pore impedance can be simplified. The spectra can be

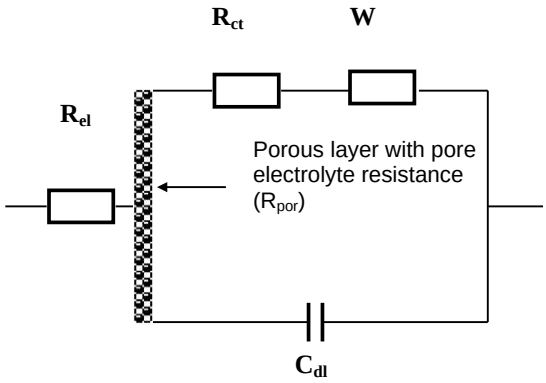

Fig. 8. Equivalent circuit (porous electrode model) for the evaluation of the impedance spectra of the silver gas-diffusion electrodes.

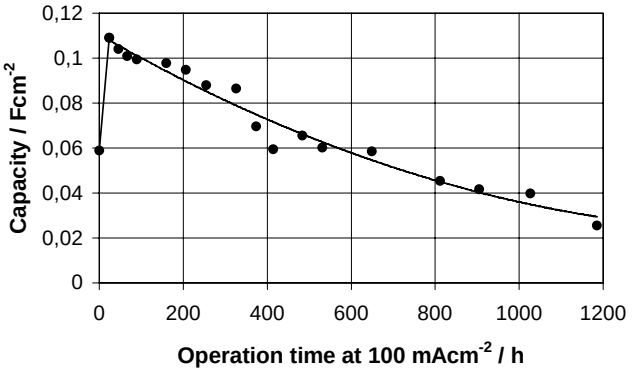

Fig. 9. Time dependence of double layer capacity obtained with a least square fit of the measured impedance spectra at open circuit potential.

simulated by an equivalent circuit (Fig. 8) consisting of a series combination of uncompensated electrolyte resistance (R_{el}) and pore impedance. The impedance of the wall surface of the pores is given by the charge transfer resistance (R_{ct}), Warburg-impedance (W) and double layer capacity (C_{dl}). The most time sensitive impedance elements are the double layer capacity, the Warburg-impedance and the charge transfer resistance. The Warburg-impedance is related to an infinite diffusion process [48–53]. From the time dependence of the impedance parameters, the aging effects can be related to the decrease of the double layer capacity (Fig. 9), a change of the porous structure and the catalyst activity (Fig. 10) and an increase of the Warburg-impedance (Fig. 11). The decrease of the capacity is given by a decrease of the electrochemically active surface. The increase of the Warburg-impedance indicates that the diffusion of reacting gas is hindered. In the Nyquist diagram one can observe the infinite diffusion as a straight line with a slope of 1 (real part = imaginary part) in the low frequency range of the spectra. In the Bode diagram due to the logarithmic scale

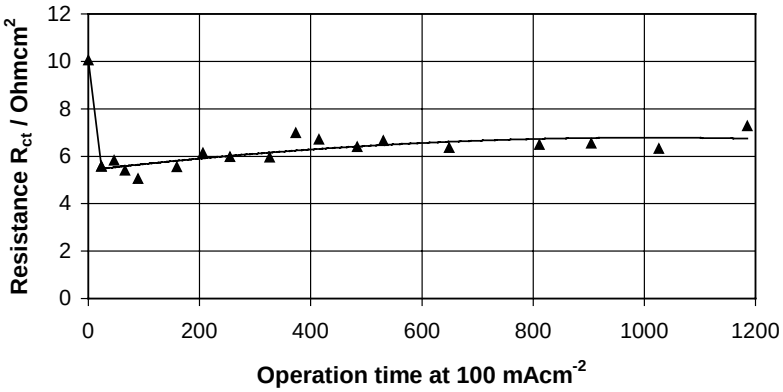

Fig. 10. Time dependence of charge transfer resistance obtained with a least square fit of the measured impedance spectra at open circuit potential.

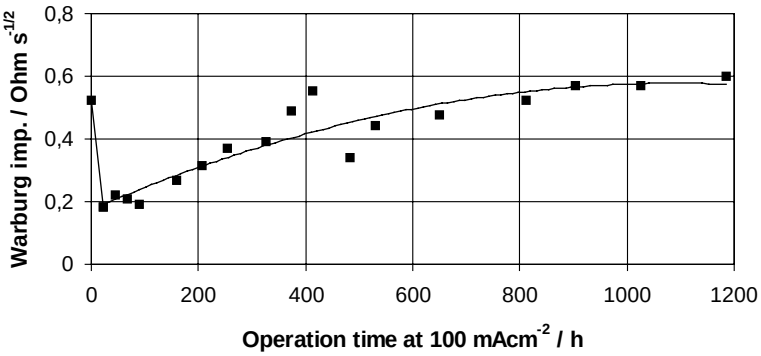

Fig. 11. Time dependence of Warburg-impedance obtained with a least square fit of the measured impedance spectra at open circuit potential.

of the impedance the diffusion can not be seen so clearly. The initial change of the impedance elements between the first and second measurement can be explained by impurities or by an oxidized surface after insertion in the test facility. Due to the transfer through the air, the electrode surfaces can easily be oxidized or be polluted. Impurities can be quickly removed by the electrochemical operation, also the oxidation state of the catalyst can quickly change in the electrochemical environmental. The surface area increases while the impurities are removed, consequently the double layer capacity increases. In addition to the active surface, the charge transfer resistance decreases, because the reaction is not hindered after removing the impurities. The initial decrease of the Warburg-impedance is correlated with an improvement of the transport processes at the beginning of the electrochemical experiments. It may be induced by a delayed penetration of the electrolyte into the electrodes or by the hindering of the transport processes within the electrode by the impurities.

4. Conclusions

During oxygen reduction at 70 °C in 30 wt.% KOH with silver GDE a decrease of the electrochemical performance is observed. The decrease of the electrochemical performance has a linear progression with a gradient of approximately $20\,\mu V\,h^{-1}$. In an operation period of 5000 h the total voltage loss will be approximately 100 mV; taking into account the higher cell voltages in AFC compared to PEFC the loss in electrochemical performance related to the cathode is approximately 12–15% of the cell voltage in 5000 h of operation time. This means that the stability of the silver cathodes is sufficient for mobile applications, but not for stationary applications. For stationary applications the long term behavior must be improved; therefore, an understanding of the degradation processes is necessary.

For the understanding of the results of the physical and electrochemical characterization two different pore systems must be distinguished: first, the pore system in the electrode formed by the space between the catalyst particles, which determines the gas transport and second the pores in the silver catalyst. In the first type of pore system the hydrophobic character is dominant.

The physical characterization of the electrodes has shown that the roughness of the catalyst decreases, consequently the surface area of the silver catalyst also decreases. The surface roughness is correlated with the second type of pore system. For Pt catalysts in PEFC fuel cells the electric field gradient was found to be the driving force for the mobility of the platinum [40]. Concerning the silver GDE, due to the hindered transport the electric field gradients are expected to be enhanced in the pores. The decrease of the surface roughing of the silver catalyst can also be explained if the electric field gradient represents also the driving force. The electrochemical characterization shows that the electrochemically active surface area related to the double layer capacity becomes smaller, which is expected from the decrease of the catalyst roughness.

As a result of the decrease of the surface roughness the pore becomes flatter and the transport hindrance in the pores in the silver catalyst decreases, as the surface in the pores also decreases. The decrease of the specific surface area concerns mainly surfaces for which the highest transport hindrance exists. Therefore, the effect of the decrease of the surface roughness on electrochemical performance is not very strong, which can also be seen in the results of the electrochemical impedance spectroscopy by the almost constant charge transfer resistance.

The second degradation effect of the electrodes observed by physical characterization is the alteration of the PTFE. The partial decomposition of the PTFE can be typically related to a loss of the degree of hydrophobicity. In the electrochemical investigation an increase of the Warburg-impedance, which is related to an increase of the transport hindrance is seen. The hydrophobic properties are important for gas transport in the electrode. The decrease of the hydrophobicity allows more pores to be flooded by the electrolyte and the transport of gas to be more hindered.

Both degradation effects mentioned above are observed with both electrochemical and physical methods. The physical methods allow an easy description of the alteration and the electrochemical methods allow a quantification of the effect on the electrochemical performance. Consequently, the combination of electrochemical and physical methods is very helpful for the study of degradation processes.

Acknowledgements

The authors thank their colleagues for experimental support, mainly Dr. Michael von Bradke for performing the SEM and REM measurements.

References

[1] G.F. McLean, T. Niet, S. Prince-Richard, N. Djilali, Int. J. Hydrogen Energy 27 (2002) 507.
[2] Internet, e.g. http://www.eyeforfuelcells.com: Astris energy in discussion with nine foreign fuel cell prospects in six countries.
[3] D.P. Davies, P.L. Adcock, M. Turpin, S.J. Rowen, J. Appl. Electrochem. 30 (2000) 101.
[4] D.P. Davies, P.L. Adcock, M. Turpin, S.J. Rowen, J. Power Sources 86 (2000) 237.
[5] B. Mattsson, H. Ericson, L.M. Torell, F. Sundfolm, Electrochim. Acta 45 (2000) 1405.
[6] G. Hübner, E. Roduner, J. Mater. Chem. 9 (1999) 409.
[7] M. Schulze, M. Lorenz, N. Wagner, E. Gülzow, Fresenius J. Anal. Chem. 365 (1999) 106.
[8] F.N. Büchi, B. Gupta, O. Haas, G.G. Scherer, Electrochim. Acta 40 (1995) 345.
[9] E. Gülzow, A. Helmbold, T. Kaz, R. Reißner, M. Schulze, N. Wagner, G. Steinhilber, J. Power Sources 86 (2000) 352.

[10] S. Gupta, D. Tryk, S.K. Zecevic, W. Aldred, D. Guo, R.F. Savinell, J. Appl. Electrochem. 28 (1998) 673.
[11] E. Gülzow, M. Fischer, A. Helmbold, R. Reißner, M. Schulze, N. Wagner, M. Lorenz, B. Müller, T. Kaz, Innovative production technique for PEFC and DMFC electrodes and degradation of MEA-components, in: Proceedings of the Fuel Cell Seminar 1998, Palm Springs, 16–19 November 1998, p. 469.
[12] E. Gülzow, T. Kaz, M. Lorenz, A. Schneider, M. Schulze, Degradation of PEFC components, in: Proceedings of the Fuel Cell Seminar 2000, Portland 30 October–2 November 2000, p. 156.
[13] M.S. Wilson, J.A. Valerio, S. Gottesfeld, Electrochim. Acta 40 (1995) 355.
[14] P.G. Dirven, W.J. Engelen, C.J.M. Van Der Poorten, J. Appl. Electrochem. 25 (1995) 122.
[15] E. Gülzow, M. Schulze, G. Steinhilber, K. Bolwin, Carbon dioxide tolerance of gas diffusion electrodes for alkaline fuel cells, in: Proceedings of the Fuel Cell Seminar, San Diego, 1994, p. 319.
[16] E. Gülzow, M. Schulze, G. Steinhilber, J. Power Sources 106 (2002) 126.
[17] S. Gultekin, M.A. Al-Saheh, A.S. Al-Zakri, K.A.A. Abbas, Int. J. Hydrogen Energy 21 (1996) 485.
[18] Y. Kiros, S. Schwartz, J. Power Sources 87 (2000) 101.
[19] S.-U. Rahman, M.A. Al-Saleh, A.S. Al-Zakri, S. Gultekin, J. Appl. Electrochem. 27 (1997) 215.
[20] M. Schulze, K. Bolwin, E. Gülzow, W. Schnurnberger, Fresenius J. Anal. Chem. 353 (1995) 778.
[21] E. Gülzow, et al., PTFE bonded gas diffusion electrodes for alkaline fuel cells, in: Proceedings of the 9th World Hydrogen Energy Conference, vol. 92, Paris, p. 1507.
[22] A. Khalidi, B. Lafage, P. Taxil, G. Gave, M.J. Clifton, P. Cezac, Int. J. Hydrogen Energy 21 (1996) 25.
[23] M. Schulze, E. Gülzow, G. Steinhilber, Appl. Surf. Sci. 179 (2001) 252.
[24] N. Wagner, E. Gülzow, M. Schulze, W. Schnurnberger, Gas diffusion electrodes for alkaline fuel cells, in: H. Steeb, H. Aba Oud (Eds.), Solar Hydrogen Energy, German–Saudi Joint Program on Solar Hydrogen Production and Utilization Phase II 1992–1995, Stuttgart 1996, ISBN 3-89100-028-6.
[25] M. Schulze, E. Gülzow, J. Power Sources 127 (2004) 252.
[26] R. Holze, Thesis, Bonn, 1983.
[27] E. Yeager, M. Razaq, D. Gervasio, A. Razaq, D. Tryk, in: Proceedings of the Workshop on Structural Effects in Electrocatalysis and Oxygen Electrochemistry, The Electrochemical Society, Pennington, NJ, 1993, p. 440.
[28] K. Rühling, C. Fischer, O. Führer, A. Winsel, Dechema Monografien, vol. 124, Verlag Chemie, Weinheim, 1991, p. 349.
[29] N. Wagner, Production and characterization of gas diffusion electrodes used to recover metals and to regenerate metal ions containing liquids from industrial plants, in: Proceedings of the 3rd European Congress of Chemical Engineering, Nürnberg, 26–28 June 2001.
[30] G. Ertl, J. Küppers, Low Energy Electron and Surface Spectroscopy, VCH Verlagsgesellschaft, Weinheim, 1985.
[31] E. Gülzow, M. Schulze, N. Wagner, T. Kaz, R. Reißner, G. Steinhilber, A. Schneider, J. Power Sources 86 (2000) 352.
[32] H. Ibach, in: H. Ibach (Ed.), Electron Spectroscopy for Surface Analysis, Springer-Verlag, Berlin, p. 5.
[33] J.J. Martínez Jubrías, M. Hidalgo, M.L. Marcos, J. González-Velasco, Surf. Sci. 366 (1996) 239.
[34] J.M. Dona, J. González-Velasco, J. Phys. Chem. 1993 (1997) 4714.
[35] J.M. Dona, J. González-Velasco, Surf. Sci. 274 (1992) 205.
[36] C. Alonso, R.C. Salvarezza, J.M. Vara, A.J. Arvia, Electrochem. Acta 35 (1990) 1331.
[37] M.L. Marcos, J. Gonzáles-Velasco, Chem. Phys. Lett. 283 (1998) 391.
[38] M. Giesen, M. Dietterle, D. Stabel, H. Ibach, D. Kolb, Surf. Sci. 384 (1997) 168.
[39] G. Andreasen, M. Nazzarro, J. Ramirez, R.C. Salvarezza, A.J. Arvia, J. Electrochem. Soc. 143 (1996) 466.
[40] M. Schulze, A. Schneider, E. Gülzow, J. Power Sources 127 (2004) 213.
[41] P. Staiti, A.S. Arico, V. Antonucci, S. Hocevar, J. Power Sources 70 (1998) 91.
[42] K. Mund, Siemens Forsch. Entwickl. Ber. 4 (1975) 68.
[43] J.P. Candy, P. Fouilloux, M. Keddam, H. Takenouti, Electrochim. Acta 27 (1982) 1585.
[44] L.M. Gassa, J.R. Vilche, M. Ebert, K. Jüttner, W.J. Lorenz, J. Appl. Electrochem. 20 (1990) 677.
[45] N. Wagner, J. Appl. Electrochem. 32 (2002) 871.
[46] H. Göhr, C.A. Schiller, Poster, in: Proceedings of the 34th ISE Meeting, Erlangen, 1983.
[47] C.A. Schiller, IM6-Software Guide, Kronach, 1994.
[48] J.R. Macdonald, D.R. Franceschetti, J. Electroanal. Chem. 307 (1991) 1.
[49] J.I. Franco, N. E Walsöe de Reca, Defect Diffusion Forum 95 (1993) 1229.
[50] D.B. Zhou, H. Vander Poorten, Electrochim. Acta 40 (1995) 1819.
[51] A. Parthasarathy, B. Dave, S. Srinivasan, A.J. Appleby, C.R. Martin, J. Electrochem. Soc. 139 (1993) 1634.
[52] D.R. Franceschetti, J.R. Macdonald, R.P. Buck, J. Electrochem. Soc. 138 (1991) 1368.
[53] C. Criado, P. Galán-Montenegro, P. Velásquez, J.R. Ramos-Barrado, J. Electroanal. Chem. 488 (2000) 59.